Study of magnetic nonlinearities in materials with low Curie temperature applied to domestic induction heating

Alberto PASCUAL [a] Jesus ACERO [a] Alexis NARVAEZ [a] and Claudio CARRETERO [b]
[a] *Department of Electronic Engineering and Communications, I3A, University of Zaragoza, María de Luna, 3, 50018 Zaragoza, Spain*
[b] *Department of Applied Physics, I3A, University of Zaragoza, Pedro Cerbuna, 12, 50009 Zaragoza, Spain*

Abstract. The analysis of the magnetic properties of alloys with low Curie temperature used in domestic induction heating is presented. These alloys allow the development of cookware with additional benefits with respect to regular cookware oriented to improve temperature control and the user's safety. Firstly, an experimental method to characterize the magnetic permeability with respect to the magnetic field strength and temperature in the material is presented. Secondly, a finite element simulation method is proposed which, considering the previous characterization, allows the calculation of the electrical equivalent of an inductor-load system as a function of temperature and magnetic field. This method makes possible the application of finite element simulation in the frequency domain with nonlinear materials, which is of interest for the design of electronics associated with domestic applications of induction heating. Simulation results are experimentally verified with various ferromagnetic alloys with low Curie temperature at different power, temperature, and operating frequency ranges.

Keywords. Domestic induction heating, electromagnetic characterization, finite element modeling

Introduction

In the last decades, domestic applications of induction heating (IH) have become very popular, as its superior advantages have been recognized by a market increasingly concerned about energy efficiency and the progressive decarbonization of society [1]. Apart from these aspects, domestic induction heating technology has been traditionally appreciated by users because of its fast dynamics and ease of cleaning [2]. Domestic induction heating technology has three main pillars [3]: magnetic elements (inductors, EMI filters), power electronic converters, and digital control and user interface. Although induction technology has reached a remarkable degree of maturity, innovations are currently being introduced especially aimed at increasing performance [4, 5], improving user safety, and enhancing the cooking experience [6, 7]. These innovations are due, among other reasons, to the use of semiconductor materials for electronic devices with improved performance or the inclusion of magnetic materials with specific properties such as low

Curie temperature alloys [8, 9]. The electromagnetic properties of the vessel materials (relative magnetic permeability and electrical conductivity) have a direct impact on the electrical equivalent circuit of the induction cooktop electromagnetic system. In general, the electrical equivalent of the inductor-load system is represented by an equivalent resistance R_{eq}, which represents the power dissipated in the system, connected in series with an equivalent inductance L_{eq}. These parameters depend on the frequency, the excitation current, the temperature of the vessel, and the B-H curve of the material among others [10]. The cooktop control electronics detect variations in the equivalent circuit of an inductor-load system, and these changes can be used for different purposes, such as automatic pot detection or protecting the user against overheating. The latter feature can be implemented with vessels manufactured with low Curie temperature [11]. The Curie temperature determines the transition of a material from its ferromagnetic phase to its paramagnetic phase, therefore, when exceeding this temperature, considerable changes in the R_{eq} and L_{eq} of the system can be detected.

Currently, there are several alloys whose electromagnetic properties, and in particular their Curie temperature, are suitable for domestic induction heating applications [12]. This temperature should be high enough to allow cooking processes such as boiling in water and frying with oil ($>100°C$), but it should be sufficiently low ($<300°C$) to protect the user in the case that, due to misuse or negligence in the cooking process, dangerous temperatures are reached. However, alloy manufacturers usually provide very little information about the magnetic performance of these materials. Usually, only the Curie temperature is provided, and other information about magnetic permeability, the dependence of permeability with the magnetic field or temperature is not available. Therefore, the simulation of domestic induction systems with these materials requires an adequate characterization of the materials in order to obtain precise results. Moreover, the simulation presents some challenges, for example, the properties of the involved materials depend on both temperature and magnetic field [13, 14]. For this purpose, the finite element method [15, 16] has been used, which can lead to convergence problems when the coupled dependence of thermal and electromagnetic simulation is considered [17].

This work proposes an experimental method to characterize magnetic alloys with low Curie temperature and a method to perform the simulation of IH systems using finite elements considering the magnetic field strength and temperature dependence of the material properties. Both the experimental characterization method and the computational model are verified through experimental results with several FeNiCrMn alloys with low Curie temperature at various frequencies and operating conditions.

1. Magnetic and thermal characterization of materials

This work considers two materials, specifically an alloy with a Curie temperature of 120ºC (Mat. A) and another alloy with a Curie temperature of 230 ºC (Mat. B). First, using EDX (energy dispersive X-ray) and SEM (scanning electron microscopy) techniques, the structure and composition of both materials were analyzed. The composition of both materials is shown in Table 1. As can be observed, even though they are alloys of the same elements (FeNiCrMn), remarkable differences are found in the composition of the materials, which will result in different magnetic properties. From the images obtained by SEM, it can be seen the microstructure of the mat. A(Fig. 1(a)) and mat. B

Table 1. Composition of the tested materials.

MATERIAL	T_{CURIE} (°C)	FORMULAE	ALLOY COMPOSITION (%)			
			Fe	Ni	Cr	Mn
Material A	120	$Fe_{66.92}Ni_{30.49}Cr_{2.14}Mn_{0.45}$	66.92	30.49	2.14	0.45
Material B	230	$Fe_{40.24}Ni_{49.03}Cr_{10.29}Mn_{0.44}$	40.24	49.03	10.29	0.44

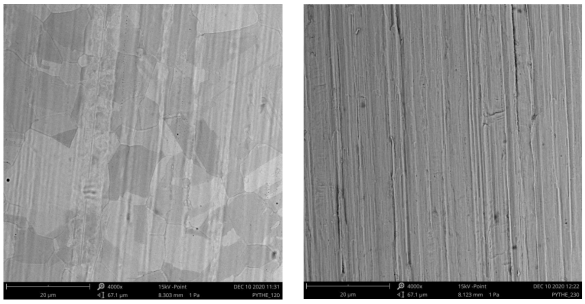

(a) (b)

Figure 1. SEM Images, microstructure: Mat. A (a) and Mat. B (b).

(Fig. 1(b)). The material A has a much coarser grain structure than B. According to [18] the more compact alloys, with finer grain size have a broader magnetization curve, so it is expected material B to be magnetically harder than material A.

The method used in this work for the magnetic and thermal characterization of the materials considered, it is based on the preliminary study presented in [19]. This study only covered up to H=150 A/m and, therefore, hardly covers the magnetic field strength (H) usually reached in domestic induction heating, between 1000 A/m and 10000 A/m. The method consists of measuring the inductance of a toroidal coil, whose magnetic core is one of the materials to be characterized. The inductance measurements and the subsequent obtention of the relative magnetic permeability are performed at different conditions of temperature, excitation current, and frequency.

The experimental setup for the magnetic characterization is shown in Fig. 2(a). It consists of a precision LCR meter (Agilent E4980A) which measures the self-inductance of the toroidal-shaped coils. This instrument has an internal oscillator whose rated power is up to 2 VA, so it allows measurements with a maximum excitation current of 100 mA. Regarding the thermal characterization, the setup also includes a custom furnace, built for that purpose, covered with an insulation blanket. The furnace temperature is set by means of a regulation system based on a proportional-integral controller, consisting of the Eurotherm 3216 controller and an SSR relay. A set of thermocouples is used to measure the temperature of the toroidal core. The temperature measures are recorded employing the Agilent 34972A data logger.

The samples of the toroidal cores have a Φ_{ext}=35 mm, Φ_{int}=23.5 mm, and t=0.5 mm, where Φ_{ext}, Φ_{int}, and t are the outer diameter, the inner diameter, and the core thickness, respectively. One of the analyzed samples is shown in Fig. 2(b). The toroid shape is appropriate to obtain the magnetic permeability by measuring the self-inductance of a device consisting of a core and a winding; since in this geometry, there is a direct rela-

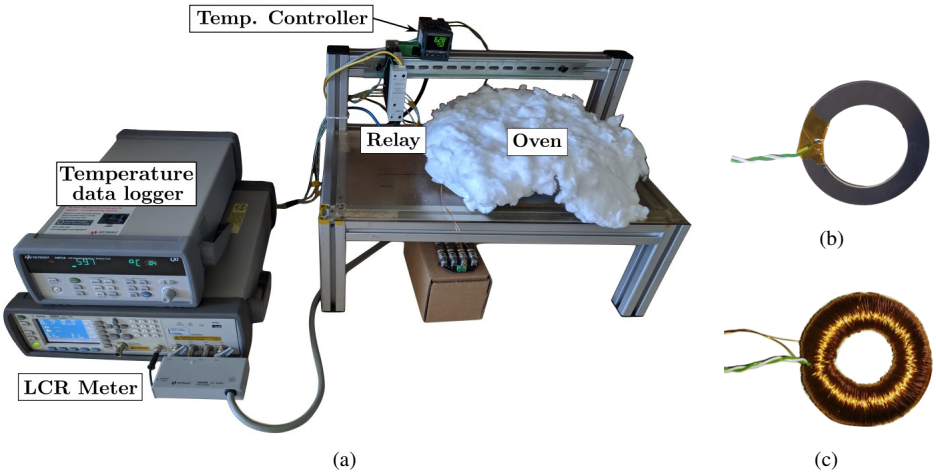

Figure 2. Elements of the experimental setup for the magnetic and thermal characterization. (a) Experimental setup. (b) Core shape. (c) Core with winding.

tionship between the winding current and the magnetic field inside the core. The winding consists of N=3500 turns of a copper strand with a diameter Φ_{Cu}=200 μm. Fig. 2(c) shows the toroidal core after the winding. Considering the dimensions of the core and the number of turns of the winding, the maximum field at the center of the toroid will be:

$$H = \frac{NI}{\pi(\Phi_{ext} + \Phi_{int})/2} \tag{1}$$

where I is the excitation current. The magnetic permeability can be deduced from the measured inductance L by means of the following expression [19]:

$$\mu_r = \frac{2\pi L}{tN^2\mu_0 \cdot \ln(\frac{\Phi_{\text{ext}}}{\Phi_{\text{int}}})} \tag{2}$$

Some characterization results are shown in Fig. 3. Fig. 3(a) shows the magnetic permeability for different magnetic field strength levels and several temperatures. As expected, the results obtained are very different for the two materials. Mat A has higher permeability and therefore saturates at a lower field. Mat. B has lower permeability and higher saturation field. Regarding the thermal characterization, Fig. 3(b) shows the relative permeability for both materials as a function of temperature for three different values of the magnetic field. As expected, the measured Curie temperature of both materials is close to that given by the manufacturer. From these results, it can also be deduced that for higher fields the dependence of the drop of the permeability with temperature is softer. It should be noted that once the maximum temperature of the experiment was reached, the samples were cooled to room temperature. Consequently, it was possible to verify that the material of the samples recovers its magnetic permeability as it cools down and moves away from its Curie temperature.

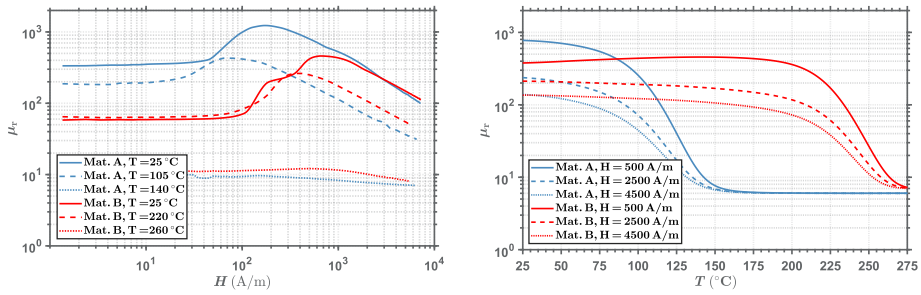

Figure 3. Results of the magnetic and thermal characterization. (a) Relative permeability at different temperatures with respect to the magnetic field. (b) Relative permeability with respect to the temperature for different magnetic fields.

As it has been observed, both materials have a good relative magnetic permeability, which allows them to be heated with induction cooktops with the same performance as the traditionally used materials. It also provides natural temperature control and protection against overheating by preventing the cookware from exceeding its Curie temperature.

2. Finite element simulation model

Domestic induction heating systems are simulated in order to obtain an electrical equivalent circuit for the inductor-load system. This circuit is required to design properly the associated power electronic converter [20] and to implement the automatic pot detection or the user protection against overheating based on impedance variations [11]. As was above commented, the electrical parameters, R_{eq} and an L_{eq}, depend on the material's electromagnetic properties, which in turn change with the H field and temperature. The analysis of magnetic systems with nonlinear materials has traditionally been approached by using finite element simulation tools [21–23]. However, papers dealing with nonlinear simulation including thermal dependence of materials in domestic IH applications are uncommon in the literature. On the other hand, the frequency-dependent analysis (which results in interest in the design of IH systems) often doesn't cover the case of non-linear materials. However, from the point of view of induction heating system design, frequency domain simulation is more useful [24] because the delivered power is usually controlled by means of the switching frequency.

In this work, it is proposed a decoupled simulation method that allows to carry out frequency-domain simulations with nonlinear magnetic materials whose properties depend on temperature. As shown in Fig. 4(a), the simulated system consists of the vessel, the inductor, a ferrite disk, and an aluminum plate placed below for shielding purposes. The model is based on the developments presented in [25]. As shown in Fig. 4(b), the peculiarity of this method is that it divides the vessel, into smaller elements, each with a different relative magnetic permeability, μ_r(T, H=H_{dis}). The μ_r function assigned in each element corresponds to the μ_r(T) functions for a given H field (H_{dis}) shown in

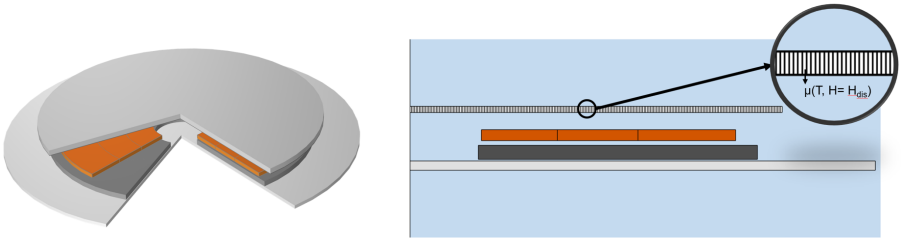

(a) (b)

Figure 4. Simulation model. (a) Domestic induction heating system comprised, from bottom to top, of aluminum shielding, ferrite disk, inductor, and vessel/load. (b) Relative permeability at each point of the material.

Fig. 3(b). The value of the magnetic field (H_{dis}) in each element is previously calculated, for various excitation currents. Thus, the simulation model consists of two steps:

- First, the magnetic field strength distribution (H_{dis}) is obtained at each point of the vessel considering the system at room temperature for each of the excitation currents to be studied. These H_{dis} results are stored for the second part of the simulation.
- Second, an algorithm is used to introduce the functions of the magnetic permeability with respect to the temperature in each of the elements of the vessel μ_r(T, H=H_{dis}). Where the H_{dis} at each element corresponds to that calculated in the previous step.

It should be noted that although the distribution of the magnetic field strength incident on the load varies as the load heats up, since its μ_r varies, the H_{dis} can be considered independent of temperature. By decoupling the problem into two steps, the model allows simulations in both, the frequency and time domains. This permits to obtain not only the parameters of the equivalent circuit at different frequencies and operating points but also the temporal evolution of the temperature in the vessel. Moreover, it avoids the problems of convergence and parameter cross-dependence that occur when directly introducing the nonlinear dependences with the H field and temperature in the finite element analysis software.

Some simulation results are shown in Fig. 5. The parameters of the study are as follows: It has been used a copper inductor with 210 mm outer diameter, 46 mm inner diameter, 22 turns and 3 mm height. A vessel whose bottom base has a height of 1 mm and a diameter of 230 mm. The materials used for the vessel correspond to those analyzed in the previous section; whose μ_r correspond to those shown in Fig. 3 and whose electrical conductivity is $1.1 \cdot 10^6$ S/m. The distance between the inductor and the load is 6 mm. Finally, the ferrite disk has an equivalent μ_r of 16, an outer diameter of 206 mm and an inner diameter of 55 mm. As shown in Fig. 5(a), although the H field and μ_r have cross dependencies, the change with temperature hardly modifies the field distribution (H_{dis}). In Fig. 5(b) it can be observed that each radial position of the load has a different magnetic permeability assigned to it, which is also affected by temperature.

Additionally, simulation results of the equivalent impedance are also shown in Fig. 6. This figure shows that the simulation model captures the dependencies of the equivalent impedance with respect to both excitation current and temperature. The temperature dis-

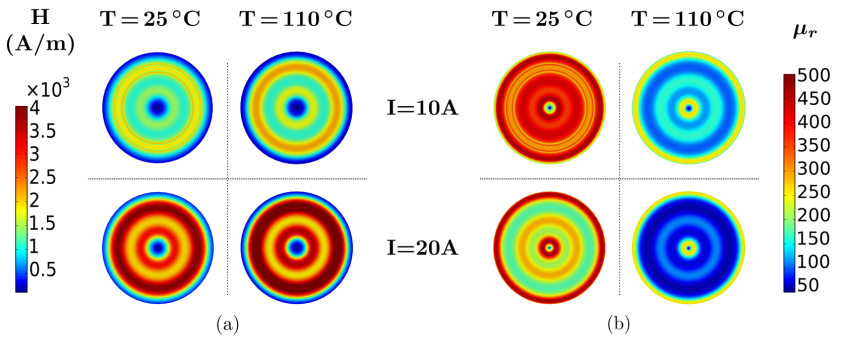

Figure 5. Simulation results at the bottom surface of the load with Mat A. (a) Magnetic field and (b) Relative magnetic permeability at different temperatures and coil excitation currents

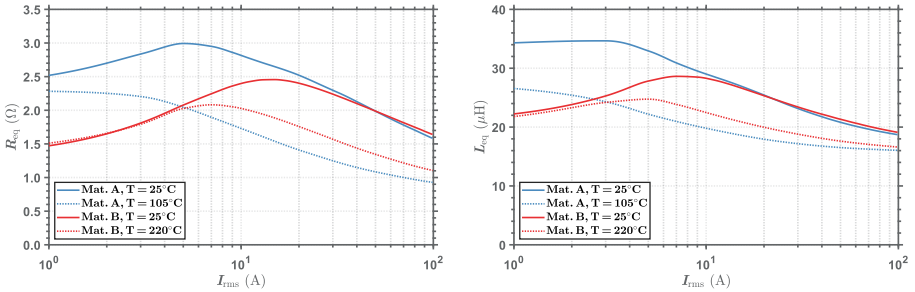

Figure 6. Simulated results of equivalent impedance with respect to the current for different temperatures at f of 35kHz. (a) Equivalent resistance. (b) Equivalent inductance.

tribution in the vessel is usually not uniform along its surface, being the areas that heat up the most the ones that have the greatest contribution to the equivalent circuit [17]; that is why the highest temperature reached in the vessel has been chosen as the reference temperature in the graphs. According to these figures, for the considered geometry the impedance drop occurs when the current is higher than 10 Amps. The changes in the equivalent impedance shown in Fig. 6 can be used for the overheating detection above mentioned.

3. Experimental results

Several experimental tests have been performed to verify the proposed simulation model. The experimental setup is shown in Fig. 7. It has been used a commercial Bosch induction cooktop to heat the material samples, a Lecroy MDA805A oscilloscope to measure the voltage and current values to obtain the equivalent circuit parameters, and a thermographic camera FLIR-A655sc to measure the temperature evolution. The purpose of

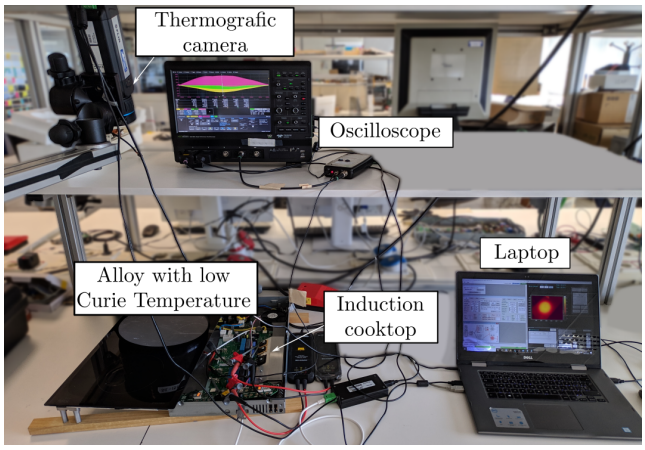

Figure 7. Elements of the experimental setup used for model validation

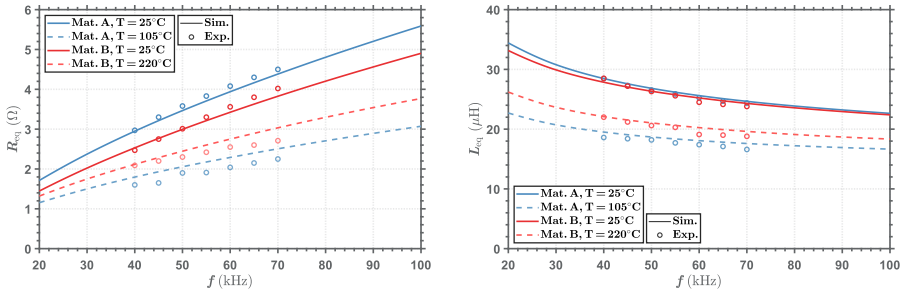

(a) (b)

Figure 8. Simulated and experimental results of equivalent impedance with respect to the frequency for different temperatures. (a) Equivalent resistance. (b) Equivalent inductance.

these tests is to obtain values of the equivalent impedance to be compared with the results of the simulation model.

Considering that cookware manufacturers do not usually provide technical information (composition, Curie temperature, electrical properties...) about their products, there may be uncertainty in the nature of the material. In order to verify the model as closely as possible, commercial cookware was not used in this study. Instead of that, 230 mm diameter disks made of a thick plate of both materials, Mat. A and Mat. B, were used. This ensures that the induction load is made of the right material. On the other hand, the disadvantage of the disks is that they have a low mass, which means that their temperature rises rapidly. For this reason, it is not possible to supply them with high power. The disks were placed on a 210 mm diameter inductor fed by the electronic stage of a commercial induction cooktop. In this converter, the power is controlled by varying the switching frequency.

The experimental results of equivalent impedance as a function of frequency for different temperatures are shown in Fig. 8. For the reasons mentioned in the previous

section, the highest temperature reached along the surface of the vessel has been chosen as the reference temperature. In addition, as already mentioned, each of the experimental frequencies corresponds to an excitation current in the coil and therefore a different H field, which has been considered in the simulation. As shown in the figures, the measure impedance tendencies follow the simulation model predictions. Moreover, the experimental results adequately match the simulations.

4. Conclusions

In this work, it has been presented a method to magnetically characterize materials as a function of temperature and H-field. In addition, a decoupled method that considers these nonlinearities has been introduced. In contrast to the linear models widely studied in the literature, which either do not consider or only take into account the dependencies of magnetic permeability on temperature or magnetic field strength, this method allows taking into account both dependencies. By comparing simulated and experimental results with the FeNiCrMn alloys with low Curie temperature, a good agreement between results has been observed. This method allows a more accurate design of the electronics associated with domestic induction heating systems that incorporate low Curie temperature materials to improve their security.

References

[1] O. Lucia, H. Sarnago, J. Acero, C. Carretero, and J. M. Burdio, "Induction heating cookers: A path towards decarbonization using energy saving cookers," *2022 International Power Electronics Conference, IPEC-Himeji 2022-ECCE Asia*, pp. 1435–1439, 2022.

[2] J. Acero, J. M. Burdio, L. A. Barragan, D. Navarro, R. Alonso, J. R. García, F. Monterde, P. Hernandez, S. Llorente, and I. Garde, "Domestic induction appliances," *IEEE Industry Applications Magazine*, vol. 16, pp. 39–47, 3 2010.

[3] E. Jang, M. J. Kwon, S. M. Park, H. M. Ahn, and B. K. Lee, "Analysis and design of flexible-surface induction-heating cooktop with gan-hemt-based multiple inverter system," *IEEE Transactions on Power Electronics*, vol. 37, pp. 12 865–12 876, 10 2022.

[4] H. Sarnago, Óscar Lucía, and J. M. Burdío, "A comparative evaluation of sic power devices for high-performance domestic induction heating," *IEEE Transactions on Industrial Electronics*, vol. 62, pp. 4795–4804, 8 2015.

[5] S. Lucia, D. Navarro, H. Sarnago, and O. Lucia, "Development of new high-performance induction heating systems using model predictive control 1," *International Journal of Applied Electromagnetics and Mechanics*, vol. 63, pp. S101–S108, 1 2020.

[6] A. Pascual, J. Acero, S. Llorente, C. Carretero, and J. Burdio, "Small-sized immersible water heaters for domestic induction heating technology," *IEEE Access*, pp. 1–1, 2023.

[7] A. Pascual, J. Acero, C. Carretero, S. Llorente, and J. M. Burdio, "Electromagnetic modeling and analysis of multimaterial cookware for domestic induction heating," *IEEE Access*, 2023.

[8] I. Astefanoaei, I. Dumitru, H. Chiriac, and A. Stancu, "Use of the fe-cr-nb-b systems with low curie temperature as mediators in magnetic hyperthermia," *IEEE Transactions on Magnetics*, vol. 50, 11 2014.

[9] ——, "Thermofluid analysis in magnetic hyperthermia using low curie temperature particles," *IEEE Transactions on Magnetics*, vol. 52, 7 2016.

[10] Q. Zhu, Q. Wu, W. Li, M. T. Pham, and L. Zhu, "A general and accurate iron loss calculation method considering harmonics based on loss surface hysteresis model and finite-element method," *IEEE Transactions on Industry Applications*, vol. 57, pp. 374–381, 1 2021.

[11] A. Pascual, J. Acero, S. Llorente, C. Carretero, and J. M. Burdio, "Self-adaptive overtemperature protection materials for safety-centric domestic induction heating applications," *IEEE Access*, vol. 11, pp. 1193–1201, 2023.

[12] T. Todaka, T. Kishino, and M. Enokizono, "Low curie temperature material for induction heating self-temperature controlling system," *Journal of Magnetism and Magnetic Materials*, vol. 320, pp. e702–e707, 10 2008.

[13] U. Lüdtke and D. Schulze, "Numerical simulation of continuous induction steel bar end heating with material properties depending on temperature and magnetic field," *IEEE Transactions on Magnetics*, vol. 34, pp. 3106–3109, 1998.

[14] M. Bullo, V. D'Ambrosio, F. Dughiero, and M. Guarnieri, "Coupled electrical and thermal transient conduction problems with a quadratic interpolation cell method approach," *IEEE Transactions on Magnetics*, vol. 42, pp. 1003–1006, 2006.

[15] P. D. Barba, F. Dughiero, E. Sieni, and A. Candeo, "Coupled field synthesis in magnetic fluid hyperthermia," *IEEE Transactions on Magnetics*, vol. 47, pp. 914–917, 2011.

[16] A. Candeo and F. Dughiero, "Numerical fem models for the planning of magnetic induction hyperthermia treatments with nanoparticles," *IEEE Transactions on Magnetics*, vol. 45, pp. 1658–1661, 3 2009.

[17] A. Pascual, J. Acero, J. M. Burdio, C. Carretero, and S. Llorente, "Electrothermal analysis of temperature-limited loads for domestic induction heating applications," *IECON Proceedings (Industrial Electronics Conference)*, vol. 2022-Octob, 2022.

[18] D. Olekšáková, P. Kollár, and J. Füzer, "Structure and magnetic properties of powdered and compacted feni alloys," *Journal of Electrical Engineering*, vol. 68, pp. 163–166, 3 2017.

[19] A. Pascual, J. Acero, C. Carretero, and S. Llorente, "Experimental characterization of materials with controlled curie temperature for domestic induction heating applications," *IECON Proceedings (Industrial Electronics Conference)*, 10 2021.

[20] P. Vishnuram, G. Ramachandiran, T. S. Babu, and B. Nastasi, "Induction heating in domestic cooking and industrial melting applications: A systematic review on modelling, converter topologies and control schemes," *Energies 2021, Vol. 14, Page 6634*, vol. 14, p. 6634, 10 2021.

[21] K. Preis, H. Stögner, and K. R. Richter, "Finite element analysis of anisotropic and nonlinear magnetic circuits," *IEEE Transactions on Magnetics*, vol. 17, pp. 3396–3398, 1981.

[22] O. A. Mohammed and W. K. Jones, "A dynamic programming - finite element procedure for the design of nonlinear magnetic devices," *IEEE Transactions on Magnetics*, vol. 26, pp. 666–669, 1990.

[23] S. Yamada, K. Bessho, and J. Lu, "Harmonic balance finite element method applied to nonlinear ac magnetic analysis," *IEEE Transactions on Magnetics*, vol. 25, pp. 2971–2973, 1989.

[24] C. Carretero, Óscar Lucia, J. Acero, R. Alonso, and J. M. Burdío, "An application of the impedance boundary condition for the design of coils used in domestic induction heating systems," *COMPEL - The International Journal for Computation and Mathematics in Electrical and Electronic Engineering*, vol. 30, pp. 1616–1625, 2011.

[25] J. Acero, R. Alonso, J. M. Burdio, L. A. Barragan, and D. Puyal, "Analytical equivalent impedance for a planar circular induction heating system," *IEEE Transactions on Magnetics*, vol. 42, pp. 84–86, 1 2006.